Flat Metamorphic InAlAs Buffer Layer on GaAs(111)A Misoriented Substrates by Growth Kinetics Control

Artur Tuktamyshev[a,b,*], Stefano Vichi[a,b], Federico Cesura[a], Alexey Fedorov[c], Sergio Bietti[a], Daniel Chrastina[d], Shiro Tsukamoto[a,e], Stefano Sanguinetti[a]

[a]*L-NESS & Department of Material Science, UNIMIB, via R. Cozzi 55, 20125 Milano, Italy*
[b]*INFN, Milano-Bicocca section, piazza della Scienza 3, 20126 Milano, Italy*
[c]*L-NESS & CNR IFN, piazza Leonardo da Vinci 32, 20133 Milano, Italy*
[d]*L-NESS & Physics Department, Polimi, Polo di Como, via Francesco Anzani 42, 22100 Como, Italy*
[e]*Present address: The University of Electro-Communications, 1-5-1 Chofugaoka, Chofu, 182-8585 Tokyo, Japan*

Abstract

We have successfully grown high quality, through the detailed control of the growth kinetics, InAlAs metamorphic buffer layers on 2°-off GaAs(111)A substrates using molecular beam epitaxy. Full plastic relaxation is obtained for a layer thickness > 40 nm. The control of adatom diffusion length and step ejection probability from the bunches, permits to reduce the InAlAs epilayer root-mean-square surface roughness to 0.55 nm.

Keywords: A1. Crystal morphology; A2. Single crystal growth; A3. Molecular beam epitaxy; B2. Semiconducting III-V materials; B3. Infrared devices

1. Introduction

Metamorphic buffer layers (MMBLs) or fully-relaxed, lattice-mismatched layers, have been intensively investigated for their application to a range of optical and electronic devices, such as solar cells [1], lasers [2], light-emitting diodes [3], transistors [4] etc. Recently, a key device emerged for quantum information technologies: quantum dot (QD) based single and entangled photon

---

*Corresponding author
Email address:* `artur.tuktamyshev@unimib.it` (Artur Tuktamyshev)

emitters operating at the telecom-wavelength band for the quantum key distribution over long distances [5, 6]. This is usually based on InAs QDs on GaAs and InP substrates and requires the use of an InGa(Al)As MMBL to obtain a long wavelength emission [7, 8, 9, 10], since the typical InAs/GaAs QD emission is around 1 μm [11, 12].

For the formation of MMBL with high crystalline and optical qualities, fundamental for the targeted device applications, the key issues are related to: i) relax the strain while minimizing the threading dislocation density, as dislocations act as effective non-radiative recombination centers [13, 14]; ii) maintain the surface root mean square (RMS) roughness to a few monolayers (MLs) to maintain the surface symmetry, to permit the fabrication of uniform 2D layers and to avoid the predominance of extrinsic nucleation centers in the QD self-assembly. Usually linear- or step-graded buffer layers and strained superlattices are commonly used to form high quality metamorphic layers on GaAs(001) substrates. These approaches require thick and complicated layer growth sequences and result in high surface roughness of few tens of nm [15], which hinder their application in practical scenarios. Recently, an approach to minimize the thickness of InGaAs MMBL on GaAs(001) has been demonstrated using nonlinear indium content grading profile. It has been shown that 180 nm-thick layer achieves full plastic relaxation [16]. T. Henksmeier *et al.* used another approach of an InGaAs epitaxial growth on GaAs(001) covered with a weekly bonded two-dimensional layer - graphene [17]. It is shown that InGaAs layers grown on graphene/GaAs(001) are more relaxed and their strain relaxation is symmetric.

In the case of InAs strained epilayers growth on (111)-oriented substrates, it has been reported that high quality lattice-relaxed MMBL can be formed, even at a large lattice mismatch, like InAs/GaAs(111)A, InAs/Si(111), and InAs/GaSb(111)A [18, 19, 20]. This is permitted by the formation of misfit dislocations at the interface starting directly from the initial stages of the growth [18]. The fast relaxation of the strain drives the system to grow two-dimensional [18, 19], thus making the fabrication of MMBL on GaAs(111)A substrates a

promising approach.

Nevertheless, the growth of MMBL on a vicinal GaAs(111)A substrate still suffers from a very low deposition rate to maintain the surface roughness low [21, 22]. This limitation is particularly relevant when the growth of thick layers is required. For instance, when it is necessary to create optical microcavities by distributed Bragg reflectors in order to increase the brightness of QD emitters [23].

In this paper we present the growth procedure to obtain a fully relaxed, thin (>40 nm) InAlAs MMBL with an atomically flat surface (RMS = 0.55 nm) grown on GaAs(111)A misoriented substrates. The use of a vicinal GaAs(111)A substrate due to step-flow growth mode permits to increase the maximum growth rate up to 0.5–1 ML/s, a typical value for the growth on GaAs(001). The flat and smooth surface morphology, which is a fundamental factor for a number of optoelectronic and electronic applications like fine structure splitting for entangled photon generation [8, 24] or a carrier mobility reduction for high-electron mobility transistors (HEMTs) [15], has been obtained through a detailed control of the growth kinetics.

2. Methods

The samples were grown on an undoped semi-insulating GaAs(111)A substrate 2°-misoriented towards ($\overline{1}\,\overline{1}\,2$) by molecular beam epitaxy (MBE). After an oxide desorption in As$_4$ flux for 5 minutes at the temperature of 590 °C a 100 nm GaAs buffer layer was grown at 520 °C with a growth rate of 0.5 ML/s (1 ML is defined as 6.26×10^{14} atoms/cm^2, the site-number density of unreconstructed GaAs(001) surface). Then the substrate temperature was decreased to grow the InAlAs MMBL. The sample growth parameters are presented in Table 1. The MMBL temperature varied from 450 to 510 °C. A 100 nm InAlAs MMBL was deposited (20 and 40 nm for samples B1 and B2, respectively). The growth rate was varied from 0.3 to 0.7 ML/s. For one sample (A1) a thin InAs interlayer (3 ML) was introduced between a GaAs buffer and an InAlAs MMBL

3

at 470 °C with a growth rate of 0.1 ML/s. During the growth of all the layers the beam equivalent pressure (BEP) of As_4 flux was about 1×10^{-5} torr.

A PANalytical X'Pert PRO MRD high resolution X-ray diffractometer (HR-XRD) equipped with a hybrid mirror and a 2-bounce Ge(220) monochromator was employed for HR-XRD measurements. The morphological characterization of the samples was performed by atomic force microscopy (AFM) in tapping mode, using tips capable of a lateral resolution of about 2 nm.

Table 1: Growth conditions of the presented samples

Sample	MMBL composition	T (°C)	Rate (ML/s)	MMBL thickness (nm)
A1	$In_{0.52}Al_{0.48}As$	470	0.5	100 (+3 ML InAs interlayer)
A2	$In_{0.52}Al_{0.48}As$	470	0.5	100
B1	$In_{0.6}Al_{0.4}As$	450	0.5	20
B2	$In_{0.6}Al_{0.4}As$	450	0.5	40
C1	$In_{0.6}Al_{0.4}As$	450	0.3	100
C2	$In_{0.6}Al_{0.4}As$	450	0.5	100
C3	$In_{0.6}Al_{0.4}As$	470	0.5	100
C4	$In_{0.6}Al_{0.4}As$	490	0.5	100
C5	$In_{0.6}Al_{0.4}As$	510	0.5	100
C6	$In_{0.6}Al_{0.4}As$	450	0.7	100

3. Results and Discussion

The heteroepitaxy on a singular GaAs(111)A substrate of an InGa(Al)As MMBL with In composition in the 50% region was demonstrated on Refs. [8] and [25]. Mano et al. [25], in order to obtain a fully relaxed MMBL, introduced a thin (4.3 ML) InAs layer between the GaAs and the InGa(Al)As MMBL. The InAs interlayer generates a network of misfit dislocations localized mainly at the InAs/GaAs interface [19, 20] which gradually relax the strain within the epilayer as the layer thickness increases [19, 25].

We applied the same strategy as the starting point of our investigation for the optimal growth condition for InAlAs MMBL on vicinal GaAs(111)A.

4

The growth conditions and the MMBL composition (sample A1) were chosen as close as possible to those reported in Ref. [25] (see Table 1). For comparison we fabricated a sample with the same InAlAs composition and thickness, but without InAs interlayer (sample A2) to assess the interlayer effectiveness also on misoriented GaAs(111)A substrates.

Figures 1a,b display a XRD reciprocal space map (RSM) for the (224) asymmetric Bragg reflection of samples A1 and A2, respectively. On both images two diffraction peaks originate from GaAs and $In_{0.52}Al_{0.48}As$. The positions of the peak are consistent, in both samples, with an indium content in the InAlAs layer of 52.0±0.4% and show an almost full relaxation of the InAlAs epilayer. Additionally, XRD shows that samples A1 and A2 have different miscut angle (although, both samples were cut from the same GaAs wafer), which explain different peak positions on Figures 1a,b for GaAs and for InAlAs, keeping the relative difference between GaAs and InAlAs peaks the same for both samples. Thus, XRD data suggest that the insertion of a thin InAs interlayer does not impact on the strain relaxation of the InAlAs layer grown on GaAs(111)A misoriented substrates.

The AFM topography of sample A1 (see Figure 2a) shows the appearance of large islands with the average lateral size and height of 602±69 and 17.8±4.9 nm, respectively, and with a density of about 7×10^6 cm^{-2}. These islands are detrimental for the optoelectronic performances of any QD based device realized on it. Instead, a fully relaxed thin InAlAs MMBL, without the InAs interlayer, is free of large islands (see Figure 2b), thus being a better substrate for any subsequent device fabrication [24]. Such discrepancy may be attributed to the presence of numerous steps at the misoriented InAs/GaAs interface. Their interaction with the misfit dislocation network may cause the formation of the observed three-dimensional defects, hindering the role of the InAs interlayer in reducing the MMBL strain.

As stated previously, one of the main applications of InGa(Al)As MMBL on GaAs(111)A is related to the fabrication of single photon and entangled photon emitters in the O-band ($\lambda = 1.31$ μm) telecommunication window based on

5

InAs QDs [8, 24]. On the basis of quantum mechanical calculation, the optimal Al content in InAlAs layer to obtain the InAs QDs with the desired emission properties is around 60% [24]. Thus, in the following, the optimal conditions to obtain a MMBL based on a $In_{0.6}Al_{0.4}As$ thin layer were investigated.

Samples B1 and B2 consist of 20 and 40 nm $In_{0.6}Al_{0.4}As$, respectively, directly grown on vicinal GaAs(111)A. HR-XRD analysis reveals the relaxation of 84% for sample B1 and the indium composition in the InAlAs layer of 62±8%. Such a big error is attributed the low XRD signal (see Figure 3a) from the thin InAlAs layer. On the other hand, sample B2 shows an almost full plastic lattice relaxation (92%) and the indium composition of 63±3% (see Figure 3b). AFM scans on Figures 3c,d displays a surface topography of the samples. For both samples the RMS roughness is similar (about 0.7 nm). Therefore, to have the InAlAs MMBL grown on vicinal GaAs(111)A with a nominal growth composition and an almost full plastic relaxation, the thickness should exceed 40 nm. Recently, Metal–Organic Vapor-Phase Epitaxial (MOVPE) 180 nm thick InGaAs MMBL on GaAs(001) was demonstrated [16]. A nonlinear indium content grading profile design was used to maximize plastic relaxation within minimal layer thickness. And 30 nm thick InGaAs layer was determined as the minimal thickness that exhibits a clear onset of relaxation (about 11%).

The surface roughness is a fundamental parameter to assess the quality of the MMBL, being a flat surface necessary to obtain high quality, defect free epilayers. Figure 4 reports the surface morphology of the sample series C1–C6. In this series we varied systematically the growth temperature in the range of 450–510 °C and the growth rate in the range of 0.3–0.7 ML/s (see Table 1) while keeping the same 100 nm thickness of InAlAs layer for the samples which is well enough to achieve full plastic relaxation. We observed a systematic reduction of the RMS surface roughness from RMS = 3.1 nm (sample C5) to RMS = 0.57 nm (sample C2) with decreasing the growth temperature. On the other hand, the surface roughness was also observed to increase with the decreasing the growth rate (samples C1, C2, and C6).

It is known that the surface of a solid under stress can exhibits a morpho-

6

logical instability, characterized by spontaneous roughening [26]. Surface steps are sometimes observed to form bunches resulting in a rougher surface. The stress induced roughening, in case of flat surfaces, requires nucleation of steps or facets, so that a flat surface is metastable rather than unstable.

The presence of macro-steps was already observed for the growth of strain-compensated layers on vicinal GaAs(001) substrates [27, 28, 29]. The formation of macro-steps is attributed to the lattice relaxation caused by the formation of large step-bunching. It is shown that the size of step bunching and related macro-steps can be controlled by the growth conditions [26, 29] or even their presence can be eliminated, in MOVPE, by using a TEGa source instead of a TMGa which gives an access to use lower substrate temperatures [29].

In our case, the MMBL is deposited on a substrate with an orientation that is 2° off the crystallographic (111)A plane. This misorientation creates a substantial density of steps that initiate the process of step bunching at the origin of the surface roughening [26].

In the samples grown at the same growth rate of 0.5 ML/s (C2–C5), a 12 nm height of a step bunching, corresponding to approximately 36 ML steps (see inset B in Figure 4 and Figure 5), are observed in sample C5, grown at the highest temperature of 510 °C. The average height of the step bunching then reduced to 2.3 nm ($\approx$7 ML steps) by decreasing the growth temperature down to 450 °C (sample C2). The step bunching was observed to depend on growth rate as well, ranging from 7.8 nm average step bunching height in sample C1 (0.3 ML/s) down to 2.2 nm (see inset A in Figure 4) in sample C6 (0.7 ML/s).

The presented phenomenology can be interpreted with the model introduced by Tersoff and coworkers [26]. It predicted that, on vicinal surfaces, a long-ranged attraction between steps takes place in strained layers, which leads to a robust step-bunching instability. Such instability is suppressed by the decreasing temperature. Decreasing the growth temperature reduces the adatom diffusion length, and, consequently, the step bunch average distance. This has the effect to decrease the step bunch size, as a smaller number of steps can contribute to the bunch. If the surface is exposed to a flux of atoms, coalescence terminates

7

at a maximum bunch size that depends on the flux, due to the increasing step ejection probability from the bunches, due to preferential adatom incorporation probability at the bottom steps of the bunch. This reduces step bunch size and roughens the terrace between two consecutive bunches by reducing the average terrace size. We analysed in detail the dependence of step bunch average distance (Sb), average terrace size (Tr) and RMS surface roughness as a function of the growth temperature and the growth rate in our sample set. As clearly shown in Figure 5, the reduction of the RMS obtained by decreasing the temperature is related to a sizeable reduction of the average bunch distance while the terrace width is roughly constant and close to the minimal terrace width due to the 2° miscut of the substrate. This observation is in agreement with a step-step interaction controlled by adatom diffusion. On the other side, the RMS reduction due to growth rate is related to a sizeable reduction of the terrace width while the average bunch distance remains constant, thus confirming that the observed reduction in the surface RMS is related to the surface roughening between bunches, an effect predicted by Tersoff [26] and due to step ejection from the bunches. In conclusion, our observations are in agreement with the theoretical predictions. Therefore, the step bunching can be substantially suppressed, in MMBL on misoriented substrates, by growth kinetics control, via a high growth rate and/or by low growth temperature.

4. Conclusions

We studied the growth of high quality InAlAs MMBLs on GaAs(111)A misoriented substrates by MBE for the implementation of single and entangled photon emitters based on InAs QDs. High quality thin $In_{0.6}Al_{0.4}As$ MMBL, 40 nm thick, were obtained showing an almost full plastic relaxation.

However, the epitaxy of InAlAs epilayer on vicinal GaAs(111)A substrates, due to the contemporary presence of strain and steps, poses additional issues related to the presence of a sizeable roughening of the surface, due to a step bunching present already at moderate temperatures. By controlling the growth

8

kinetics, through substrate temperature and group III flux, it was possible to reduce the surface roughness (RMS = 0.55 nm). The optimal growth conditions were T = 450 °C and the growth rate of 0.7 ML/s.

5. Declaration of Interests

[210] The authors declare that they have no known competing financial interests or personal relationships that could have appeared to influence the work reported in this paper.

6. Acknowledgements

References

[1] R. M. France, F. Dimroth, T. J. Grassman, R. R. King, Metamorphic [220] epitaxy for multijunction solar cells, MRS Bulletin 41 (2016) 202–209. `doi: 10.1557/mrs.2016.25`.

[2] E. Tournié, L. Cerutti, J.-B. Rodriguez, H. Liu, J. Wu, S. Chen, Metamorphic III–V semiconductor lasers grown on silicon, MRS Bulletin 41 (2016) 218–223. `doi:10.1557/mrs.2016.24`.

[225] [3] Q. Lu, A. Marshall, A. Krier, Metamorphic integration of GaInAsSb material on GaAs substrates for light emitting device applications, Materials 12 (2019) 1743. `doi:10.3390/ma12111743`.

[4] K. E. Lee, E. A. Fitzgerald, Metamorphic transistors: building blocks for hetero-integrated circuits, MRS Bulletin 41 (2016) 210–217. `doi:10.1557/ [230] mrs.2016.27`.

9

[5] A. Orieux, M. A. M. Versteegh, K. D. Jöns, S. Ducci, Semiconductor devices for entangled photon pair generation: a review, Reports on Progress in Physics 80 (2017) 076001. `doi:10.1088/1361-6633/aa6955`.

[6] D. Huber, M. Reindl, J. Aberl, A. Rastelli, R. Trotta, Semiconductor quantum dots as an ideal source of polarization-entangled photon pairs on-demand: a review, Journal of Optics 20 (2018) 073002. `doi:10.1088/2040-8986/aac4c4`.

[7] E. S. Semenova, R. Hostein, G. Patriarche, O. Mauguin, L. Largeau, I. Robert-Philip, A. Beveratos, A. Lemaître, Metamorphic approach to single quantum dot emission at 1.55 μm on GaAs substrate, Journal of Applied Physics 103 (2008) 103533. `doi:10.1063/1.2927496`.

[8] N. Ha, T. Mano, T. Kuroda, K. Mitsuishi, A. Ohtake, A. Castellano, S. Sanguinetti, T. Noda, Y. Sakuma, K. Sakoda, Droplet epitaxy growth of telecom InAs quantum dots on metamorphic InAlAs/GaAs(111)A, Japanese Journal of Applied Physics 54 (2015) 04DH07. `doi:10.7567/JJAP.54.04DH07`.

[9] S. L. Portalupi, M. Jetter, P. Michler, InAs quantum dots grown on metamorphic buffers as non-classical light sources at telecom C-band: a review, Semiconductor Science and Technology 34 (2019) 053001. `doi:10.1088/1361-6641/ab08b4`.

[10] W. Zhan, S. Ishida, J. Kwoen, K. Watanabe, S. Iwamoto, Y. Arakawa, Emission at 1.6 μm from InAs quantum dots in metamorphic InGaAs matrix, Physica Status Solidi B 257 (2020) 6710–6716. `doi:10.1002/pssb.201900392`.

[11] W.-H. Chang, W. Y. Chen, T. M. Hsu, N.-T. Yeh, J.-I. Chyi, Hole emission processes in InAs/GaAs self-assembled quantum dots, Physical Review B 66 (2002) 195337. `doi:10.1103/PhysRevB.66.195337`.

10

[12] M. Souaf, M. Baira, O. Nasr, M. H. H. Alouane, H. Maaref, L. Sfaxi, B. Ilahi, Investigation of the InAs/GaAs quantum dots' size: dependence on the strain reducing layer's position, Materials 8 (2015) 4699–4709. `doi: 10.3390/ma8084699`.

[13] J. K. Richardson, M. L. Lee, Metamorphic epitaxial materials, MRS Bulletin 41 (2016) 193–198. `doi:10.1557/mrs.2016.7`.

[14] Y. B. Bolkhovityanov, O. P. Pchelyakov, S. I. Chikichev, Silicon-germanium epilayers: physical fundamentals of growing strained and fully relaxed heterostructures, Physics-Uspekhi 44 (2001) 655–680. `doi:10.1070/PU2001v044n07ABEH000879`.

[15] D. Kohen, X. S. Nguyen, S. Yadav, A. Kumar, R. I. Made, C. Heidelberger, X. Gong, K. H. Lee, K. E. K. Lee, Y. C. Yeo, S. F. Yoon, E. A. Fitzgerald, Heteroepitaxial growth of $In_{0.30}Ga_{0.70}As$ high-electron mobility transistor on 200 mm silicon substrate using metamorphic graded buffer, AIP Advances 6 (2016) 085106. `doi:10.1063/1.4961025`.

[16] R. Sittig, C. Nawrath, S. Kolatschek, S. Bauer, R. Schaber, J. Huang, P. Vijayan, P. Pruy, S. L. Portalupi, M. Jetter, P. Michler, Thin-film In-GaAs metamorphic buffer for telecom C-band InAs quantum dots and optical resonators on GaAs platform, Nanophotonics 11 (2022) 1109–1116. `doi:10.1515/nanoph-2021-0552`.

[17] T. Henksmeier, J. F. Schulz, E. Kluth, M. Feneberg, R. Goldhahn, A. M. Sanchez, M. Voigt, G. Grundmeier, D. Reuter, Remote epitaxy of $In_xGa_{1-x}As$ (001) on graphene covered GaAs (001) substrates, Journal of Crystal Growth 593 (2022) 126756. `doi:10.1016/j.jcrysgro.2022.1267562`.

[18] H. Yamaguchi, J. G. Belk, X. M. Zhang, J. L. Sudijono, M. R. Fahy, T. S. Jones, D. W. Pashley, B. A. Joyce, Atomic-scale imaging of strain

²⁸⁵ relaxation via misfit dislocations in highly mismatched semiconductor heteroepitaxy: InAs/GaAs(111)A, Physical Review B 55 (1997) 1337–1340. `doi:10.1103/PhysRevB.55.1337`.

[19] A. Ohtake, M. Ozeki, Strain relaxation in InAs/GaAs(111)A heteroepitaxy, Physical Review Letters 84 (2000) 4665–4668. `doi:10.1103/PhysRevLett.84.4665`.

[20] A. Ohtake, T. Mano, Y. Sakuma, Strain relaxation in InAs heteroepitaxy on lattice- mismatched substrates, Scientific Reports 10 (2020) 4606. `doi:10.1038/s41598-020-61527-9`.

[21] L. Esposito, S. Bietti, A. Fedorov, R. Nötzel, S. Sanguinetti, Ehrlich-Schwöbel effect on the growth dynamics of GaAs(111)A surfaces, Physical Review Materials 1 (2017) 024602. `doi:10.1103/PhysRevMaterials.1.024602`.

[22] F. Herzog, M. Bichler, G. Koblmüller, S. Prabhu-Gaunkar, W. Zhou, M. Grayson, Optimization of AlAs/AlGaAs quantum well heterostructures on on-axis and misoriented GaAs (111)B, Applied Physics Letters 100 (2012) 192106. `doi:10.1063/1.4711783`.

[23] O. Gazzano, G. S. Solomon, Toward optical quantum information processing with quantum dots coupled to microstructures, Journal of the Optical Society of America B 33 (2016) C160–C175. `doi:10.1364/JOSAB.33.00C160`.

[24] A. Tuktamyshev, A. Fedorov, S. Bietti, S. Vichi, K. D. Zeuner, K. D. Jöns, D. Chrastina, S. Tsukamoto, V. Zwiller, M. Gurioli, S. Sanguinetti, Telecom-wavelength InAs QDs with low fine structure splitting grown by droplet epitaxy on GaAs(111)A vicinal substrates, Applied Physics Letters 118 (2021) 133102. `doi:10.1063/5.0045776`.

[25] T. Mano, K. Mitsuishi, N. Ha, A. Ohtake, A. Castellano, S. Sanguinetti, T. Noda, Y. Sakuma, T. Kuroda, K. Sakoda, Growth of metamorphic

12

InGaAs on GaAs(111)A: counteracting lattice mismatch by inserting a thin InAs interlayer, Crystal Growth & Design 16 (2016) 5412–5417. `doi:10.1021/acs.cgd.6b00899`.

[26] J. Tersoff, Y. H. Phang, Z. Zhang, M. G. Lagally, Step-bunching instability of vicinal surfaces under stress, Physical Review Letters 75 (1995) 2730–2733. `doi:10.1103/PhysRevLett.75.2730`.

[27] C. Giannini, L. Tapfer, Y. Zhuang, L. D. Caro, T. Marschner, W. Stolz, Structural ordering and interface morphology in symmetrically strained (GaIn)As/Ga(PAs) superlattices grown on off-oriented GaAs(100), Physical Review B 55 (1997) 5276–5283. `doi:10.1103/PhysRevB.55.5276`.

[28] D. Alonso-Álvarez, T. Thomas, M. Führer, N. P. Hylton, N. J. Ekins-Daukes, D. Lackner, S. P. Philipps, A. W. Bett, H. Sodabanlu, H. Fujii, K. Watanabe, M. Sugiyama, L. Nasi, M. Campanini, InGaAs/GaAsP strain balanced multiquantum wires grown on misoriented GaAs substrates for high efficiency solar cells, Applied Physics Letters 105 (2014) 083124. `doi:10.1063/1.4894424`.

[29] H. Fujii, H. Sodabanlu, M. Sugiyama, Y. Nakano, Low-temperature MOVPE using TEGa for suppressed layer undulation in $In_xGa_{1-x}As/GaAs_{1-y}P_y$ superlattice on vicinal substrates, Journal of Crystal Growth 414 (2014) 3–9. `doi:10.1016/j.jcrysgro.2014.10.043`.
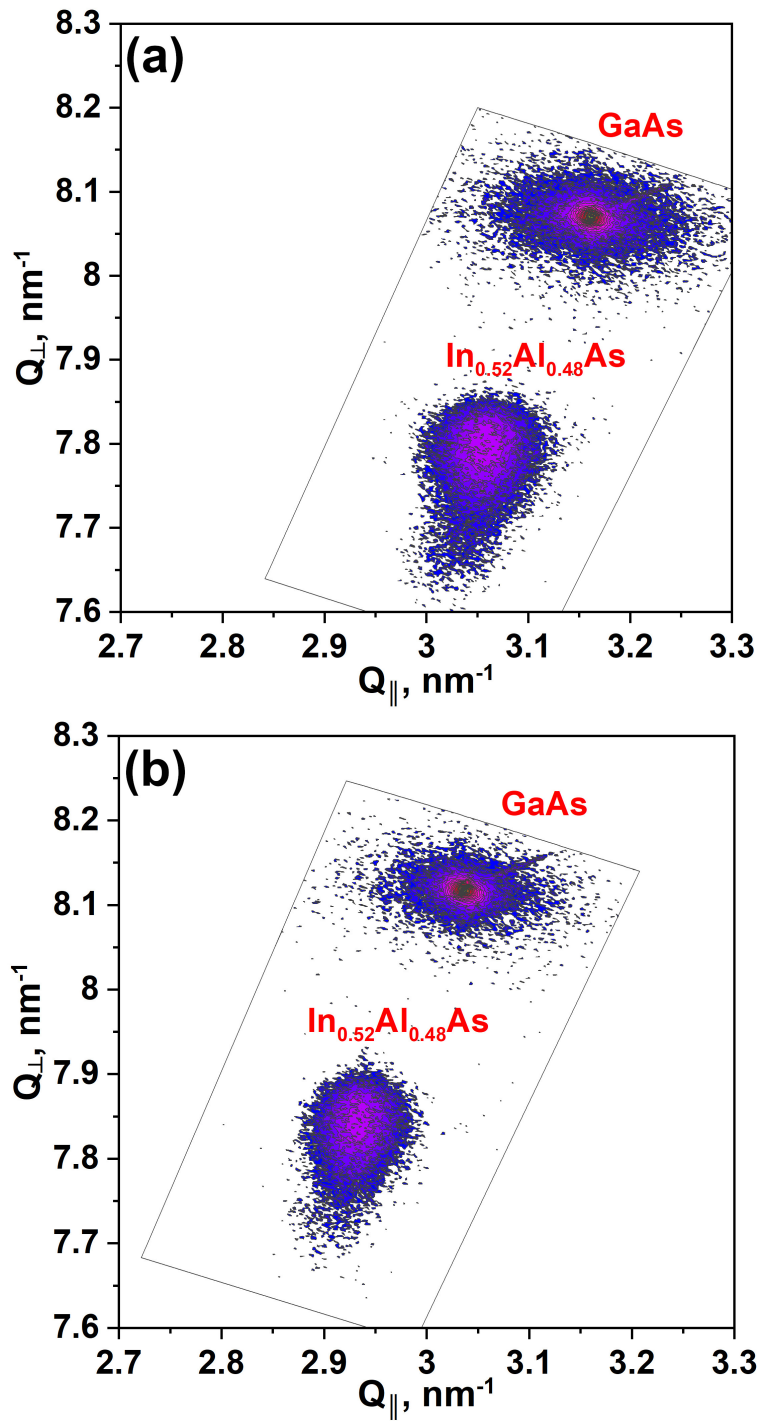
13

Figure 1: XRD RSM, taken around the (224) asymmetric Bragg reflection of (a) sample A1 and (b) sample A2. The shift of the peak positions for GaAs and for InAlAs is related to different miscut angle of the samples.
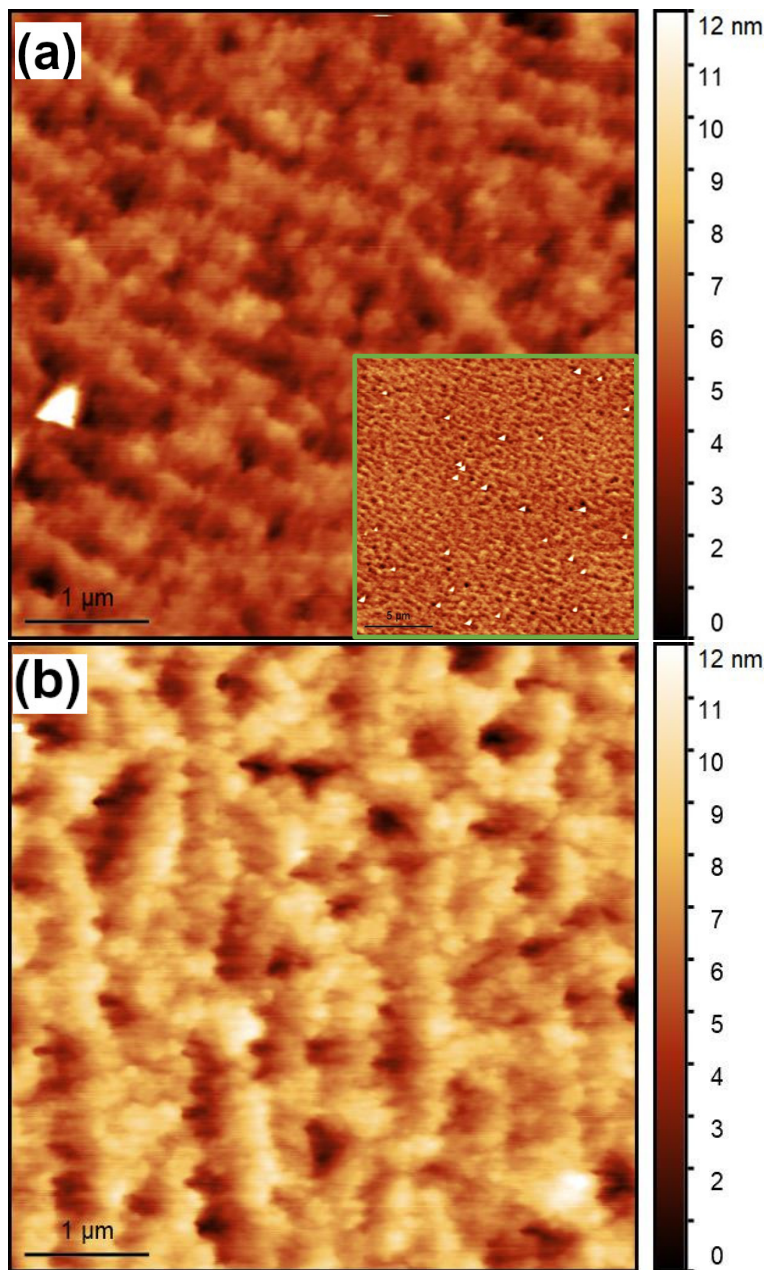
14

Figure 2: AFM topography images of (a) sample A1 (5×5 μm^2) and (b) sample A2 (5×5 μm^2). The inset in (a) shows 20×20 μm^2 AFM topography image of sample A1 with the presence of large islands.
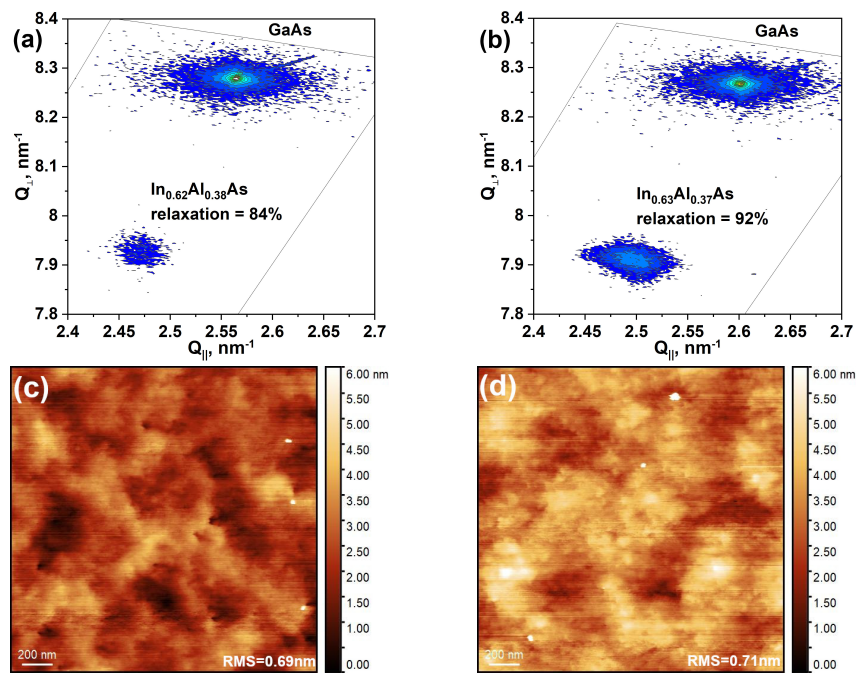
Figure 3: XRD RSM, taken around the (224) asymmetric Bragg reflection of (a) sample B1 and (b) sample B2. (c),(d) Their 2×2 $\mu\mathrm{m}^2$ AFM topography images, respectively.
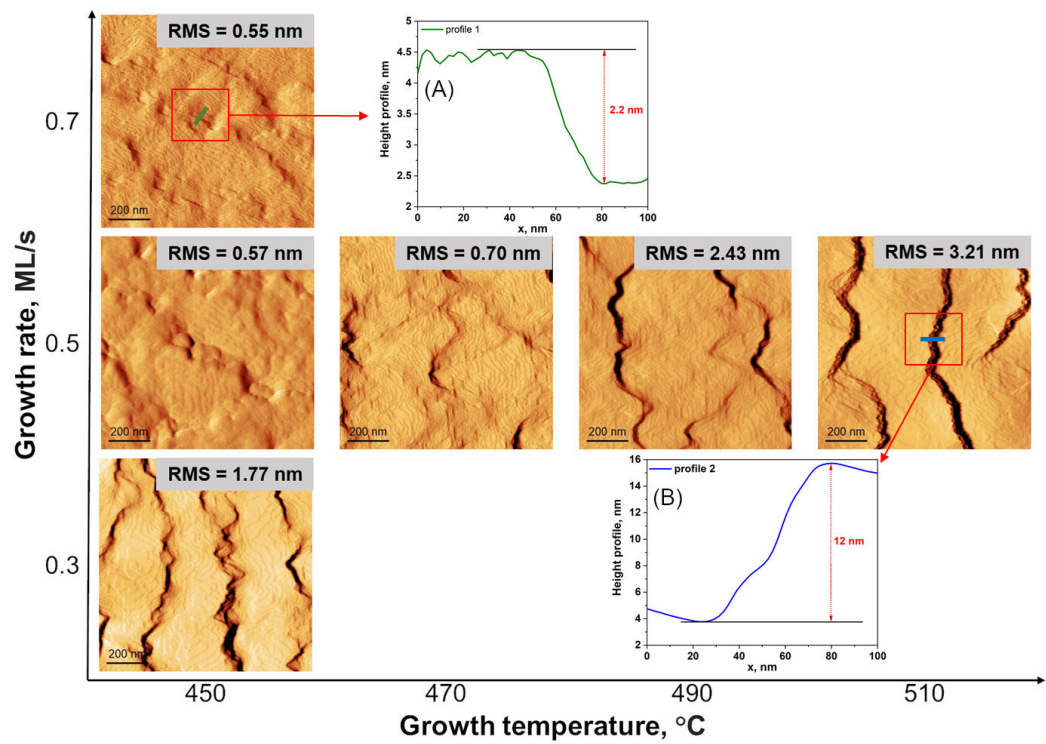
Figure 4: AFM images of the sample series C1–C6 showing the influence of the growth conditions on the morphology of an $In_{0.6}Al_{0.4}As$ layer directly grown on vicinal GaAs(111)A. Inset A: line scan of the sample B6 along the green line. Inset B: line scan of the sample B5 along the green line.
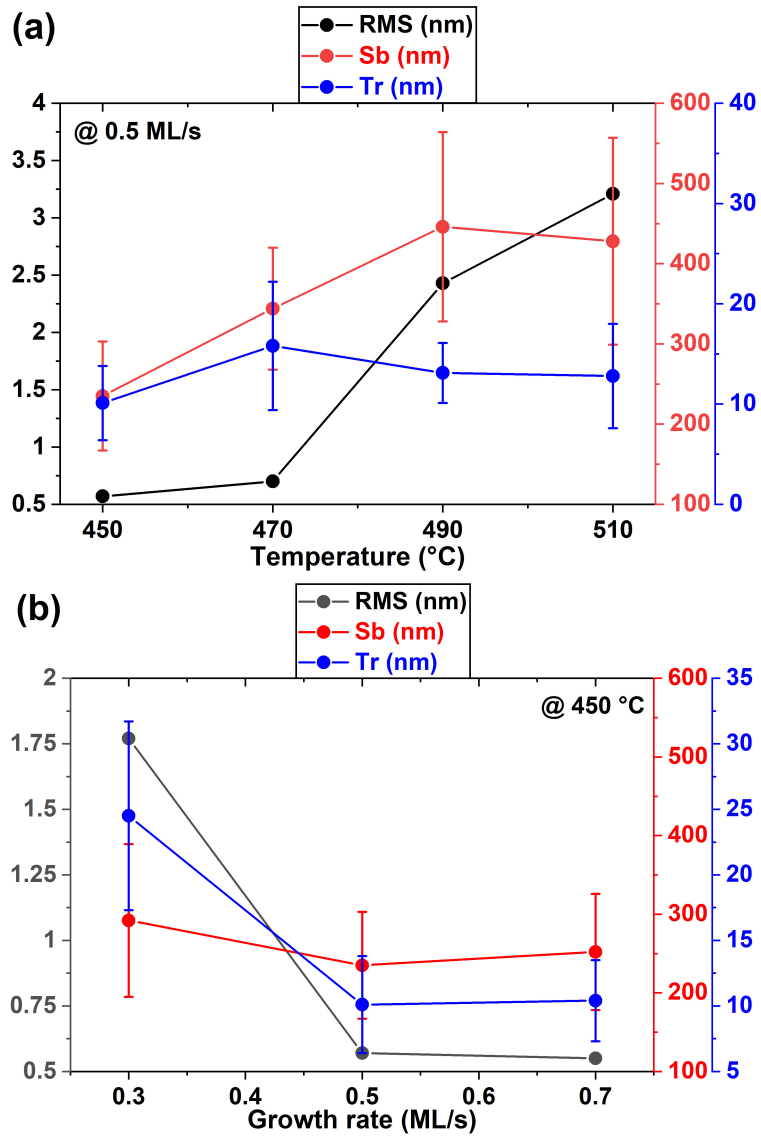
Figure 5: Dependence of RMS (black dots), average step bunch distance - Sb (red dots), and the terrace width - Tr (blue dots) for samples C1–C6. Panel (a): the temperature dependence at fixed growth rate of 0.5 ML/s (samples C2-C5). Panel (b): the growth rate dependence at fixed temperature of T = 450 °C (samples C1, C2, and C6). All the vertical scales are in nm. The minimal step terrace width for fully relaxed $In_{0.6}Al_{0.4}As$ in case of 2° miscut = 9.74 nm.